NACA

RESEARCH MEMORANDUM

TRANSONIC FLIGHT TESTS TO COMPARE THE ZERO-LIFT DRAGS OF UNDERSLUNG NACELLES VARIED SPANWISE ON A 45° SWEPTBACK WING AND BODY COMBINATION

By Sherwood Hoffman

Langley Aeronautical Laboratory
Langley Field, Va.

NATIONAL ADVISORY COMMITTEE
FOR AERONAUTICS

WASHINGTON

July 1, 1952

Classification cancelled (or changed to Unclassified)

By Authority of NASA Tech Pub Announcement #94
(OFFICER AUTHORIZED TO CHANGE)

13 Apr 56

By .....
NAME

.....
GRADE OF OFFICER MAKING CHANGE)

6 Apr 61
DATE

NATIONAL ADVISORY COMMITTEE FOR AERONAUTICS

RESEARCH MEMORANDUM

TRANSONIC FLIGHT TESTS TO COMPARE THE ZERO-LIFT DRAGS OF UNDERSLUNG NACELLES VARIED SPANWISE ON A 45° SWEPTBACK WING AND BODY COMBINATION

By Sherwood Hoffman

SUMMARY

The effect on zero-lift drag of varying the location of an underslung nacelle along the semispan of a transonic research vehicle has been determined through rocket-propelled flight tests between Mach numbers of 0.8 and 1.25. The wing had a sweepback angle of 45° along the quarter-chord line, an aspect ratio of 6.0, a taper ratio of 0.6, and an NACA 65A009 airfoil section in the free-stream direction. The nacelle was mounted in a fixed chordwise position and was successively located at 18, 40, and 96 percent of the semispan. The nacelle and fuselage fineness ratios were 9.66 and 10.0, respectively.

The nacelle located at the wing tip had the lowest drag, due to favorable interference effects, throughout the Mach number range. When nacelles were located at either the 18- or 40-percent station, large unfavorable interference effects were obtained above a Mach number of 0.93. No unfavorable interference effects were obtained between Mach numbers of 0.8 and 0.93 for any of the nacelle positions investigated. A large reduction in nacelle-plus-interference drag was obtained near a Mach number of 1.0 by moving the underslung nacelles vertically to symmetrically mounted positions. The drag-rise Mach number of the basic configuration was reduced from 0.96 to 0.94 by mounting underslung nacelles at the wing tips and to 0.90 by locating the nacelles inboard on the wing.

INTRODUCTION

As part of a general transonic research program of the National Advisory Committee for Aeronautics to investigate the aerodynamic properties of promising aircraft configurations, the Langley Pilotless Aircraft Research Division (at its testing station at Wallops Island, Va.) has tested a series of rocket-propelled free-flight models to

determine the effect of nacelle location on the zero-lift drag of a high-aspect-ratio, 45° sweptback wing and body combination. Previous papers (refs. 1 to 4) show the variations of zero-lift drag coefficient and nacelle-plus-interference drag coefficient with Mach number for a solid nacelle in various symmetrical positions on the semispan, vertical and chordwise positions at 40-percent semispan, and several chordwise positions at the wing tip. Reference 5 shows the effect of aspect ratio on the nacelle drags for nacelles located at the wing tips. The present paper gives a comparison of the drags at zero lift obtained for an underslung nacelle tested in three semispan locations on the high-aspect-ratio wing and body used in the foregoing investigations.

The nacelles were proportioned to house an axial-flow turbojet engine with an afterburner. The basic lines of the nacelle nose were designed to accommodate NACA 1-series nose inlets with critical Mach numbers above 0.9.

The nacelles were made solid, by fairing the nose inlet to a point, on the premise that the nacelle-plus-interference drag would be about the same for the solid and ducted nacelles at corresponding Mach numbers. Subsequent tests of the solid and ducted nacelles, designed for a mass-flow ratio of about 0.7, in wing-tip locations (ref. 6) show that making the nacelle solid in the manner prescribed had a negligible effect on the nacelle-plus-interference drag throughout the test range.

Flight tests covered a continous speed range varying between Mach numbers of 0.8 and 1.25. The Reynolds number, based on wing mean aerodynamic chord, varied from 3.8×10^6 to 7.3×10^6.

SYMBOLS

a	tangential acceleration, ft/sec^2
b	wing span, ft
C_D	total drag coefficient, based on S_W
C_{D_N}	drag coefficient for nacelle plus interference, based on S_F
g	acceleration due to gravity, 32.2 ft/sec^2
M	Mach number
q	free-stream dynamic pressure, lb/sq ft

[redacted]

R	Reynolds number, based on total wing mean aerodynamic chord
S_F	frontal area of one nacelle, sq ft
S_W	total wing plan-form area, sq ft
W	weight of model after burnout, lb
Y	distance between nacelle center line and fuselage center line, ft
γ	angle between flight path and horizontal, deg

MODELS

The models used for this investigation were the same as those in references 1 to 6 except for the location of the nacelles. Details and dimensions of the wing-body-fin combination, the solid nacelle, and the nacelle positions are given in figures 1, 2, and 3. Coordinates of the fuselage, airfoil section, and nacelle are given in reference 1. Photographs showing the general arrangements of the models tested are presented as figure 4.

The wing had a sweepback angle of 45° along the quarter-chord line, an aspect ratio of 6.0 (based on total wing plan-form area), a taper ratio of 0.6, and an NACA 65A009 airfoil section in the free-stream direction. The leading edge of the wing intersected the fuselage contour at the maximum-diameter station. The fuselage fineness ratio was 10.0. The ratio of total wing plan-form area to fuselage frontal area was 16.0.

Each nacelle was a solid body of revolution having an NACA 1-50-250 nose-inlet profile, a cylindrical midsection, and an afterbody with the proportions of form 111 of reference 7. The inlet was faired to a point, in order to make the nacelle solid. The fineness ratio of the solid nacelle was 9.66.

The nacelles were mounted in underslung positions on the wing, in the free-stream direction, and were successively located at 18, 40, and 96 percent of the semispan (fig. 3). The distance between the pointed nose of the nacelle and the maximum thickness of the local wing chord (40-percent-chord line) was kept constant and equal to that used in reference 1 for symmetrically mounted nacelles. For each nacelle position tested, the underslung nacelles were attached to opposite surfaces of each wing panel as is shown in figure 4(b). This asymmetric arrangement was used so that any trim change would produce roll rather than

[redacted]

pitch and the model would fly at essentially zero lift. No filleting was employed at the nacelle-wing junctures.

TESTS AND MEASUREMENTS

The rocket-propelled zero-lift models were tested at the Langley Pilotless Aircraft Research Station at Wallops Island, Va. Each model was propelled by a two-stage rocket system (as described in ref. 2) and launched from a rail launcher (fig. 4(a)). Velocity and trajectory data were obtained from the CW Doppler velocimeter and the NACA modified SCR 584 tracking radar unit, respectively. A survey of atmospheric conditions for each test was made through radiosonde measurements from an ascending balloon.

The flight tests covered a continuous Mach number range from low-supersonic to high-subsonic speeds. The maximum Mach numbers attained by the flight models varied between 1.12 and 1.25. The Reynolds number, based on wing mean aerodynamic chord, varied from approximately 3.8×10^6 to 7.3×10^6 over the test range as is shown in figure 5.

Values of total drag coefficient, based on total wing plan-form area, were calculated for decelerating flight with the relationship

$$C_D = -\frac{W}{qgS_W}(a + g \sin \gamma)$$

The variations of nacelle-plus-interference drag coefficient with Mach number were obtained from the difference in drag coefficient of faired C_D curves of a model with nacelles and the model without nacelles (ref. 2). This coefficient, based on nacelle frontal area, is

$$C_{D_N} = \left(C_{D_{\text{nacelles on}}} - C_{D_{\text{nacelles off}}}\right)\frac{S_W}{2S_F}$$

where $C_{D_{\text{nacelles on}}}$ and $C_{D_{\text{nacelles off}}}$ are based on S_W.

The magnitude of the error in drag coefficient was established from the test results of three identical models without nacelles in reference 2 and was based on the maximum deviation found between curves faired through the experimental points. At Mach numbers less than 0.93 and

greater than 1.02, the errors in total drag coefficient, nacelle-plus-interference drag coefficient, and Mach number are believed to be within the following limits:

C_D	±0.0004
C_{D_N}	±0.046
M	±0.005

Near Mach number 1.0, where the slope of the drag curve changes rapidly, the errors in drag coefficient are larger than in the foregoing table and are believed to be less than the following:

C_D	±0.001
C_{D_N}	±0.1

RESULTS AND DISCUSSION

Faired curves showing the variations of total drag coefficient with Mach number for the models tested are presented in figure 6. The curve for the configuration without nacelles was obtained from reference 2 and is an average C_D curve for three identical models of the wing-body-fin combination (model A) used herein. A comparison of the drag curves shows that the model with nacelles at the wing tips (model D) had less drag than the other models with nacelles (models B and C) through most of the test range. Near Mach number 1.0, C_D from model D was about equal to the drag coefficient of the model without nacelles and about 0.01 lower than the C_D of the models with nacelles located at either the 18- or 40-percent-semispan stations. The subsonic drag coefficients of all the models were approximately equal up to a Mach number 0.9. The drag-rise Mach number of the basic configuration was reduced from 0.96 to 0.94 by adding nacelles to the wing tips and to 0.90 by locating the nacelles inboard on the wing.

The variations of nacelle-plus-interference drag coefficient with Mach number in figure 6 are compared with the estimated drag coefficient of an isolated nacelle. The drag coefficient for the isolated nacelle was estimated in reference 2 from theoretical and experimental data at various Mach numbers through the test range. From a comparison of the variations of C_{D_N} with Mach number, it is evident that favorable interference effects were obtained throughout the range when the nacelles were located at the wing tips. Moving the nacelles inboard to either the 18- or 40-percent-semispan stations resulted in large unfavorable interference effects above a Mach number of 0.93. No unfavorable

[redacted]

interference effects were indicated for any of the nacelle positions tested at Mach numbers less than 0.93.

Figure 7 gives the variations of the nacelle-plus-interference drag coefficients with nacelle location along the semispan at Mach numbers of 0.9, 1.0, and 1.1 for the underslung nacelles and, from reference 1, for the nacelles mounted symmetrically about the local wing chord. At Mach numbers of 1.0 and 1.1, the comparison shows that the variations of C_{D_N} with spanwise nacelle location were similar for the underslung and symmetrical nacelles and that a large reduction in nacelle drag could be obtained by mounting the underslung nacelles symmetrically about the local wing chord. The variations of C_{D_N} with $\frac{Y}{b/2}$ for both the underslung and symmetrical positions were possibly due to interference effects between the nacelles and fuselage, particularly for the inboard locations, as indicated in reference 8. It is believed, however, that interference between the wing and nacelles was responsible for the large reduction in nacelle drag obtained by moving the underslung nacelles vertically to symmetrical positions. At a Mach number of 0.9, both underslung and symmetrical nacelle positions had about the same drag regardless of nacelle location on the semispan. From these tests, it is apparent that, at Mach numbers greater than 0.9, the drag increment associated with adding nacelles to a wing-body combination is largely dependent on the nacelle location.

CONCLUSIONS

The effect on zero-lift drag of varying the location of an underslung nacelle along the semispan of a 45° sweptback wing and body combination has been determined through flight tests of rocket-propelled models between Mach numbers of 0.8 and 1.25. The nacelle was mounted in a fixed chordwise position and was successively located at 18, 40, and 96 percent of the semispan for the tests. The nacelle had a fineness ratio of 9.66. The following effects were noted:

1. The nacelle located at the wing tip had the lowest drag, due to favorable interference effects, throughout the Mach number range. When nacelles were located at either the 18- or 40-percent station, large unfavorable interference effects were obtained above a Mach number of 0.93. No unfavorable interference effects were obtained between Mach numbers of 0.80 and 0.93 for any of the nacelle positions investigated.

2. A large reduction in nacelle-plus-interference drag was obtained near a Mach number of 1.0 by moving the underslung nacelle vertically

to a symmetrically mounted position about the local wing chord, regardless of spanwise location of the nacelle.

3. The drag-rise Mach number of the basic configuration was reduced from 0.96 to 0.94 by mounting the underslung nacelles at the wing tips and to 0.90 by locating the nacelles inboard on the wing.

Langley Aeronautical Laboratory
National Advisory Committee for Aeronautics
Langley Field, Va.

REFERENCES

1. Pepper, William B., Jr., and Hoffman, Sherwood: Comparison of Zero-Lift Drags Determined by Flight Tests at Transonic Speeds of Symmetrically Mounted Nacelles in Various Spanwise Positions on a 45° Sweptback Wing and Body Combination. NACA RM L51D06, 1951.

2. Pepper, William B., Jr., and Hoffman, Sherwood: Transonic Flight Tests to Compare the Zero-Lift Drag of Underslung and Symmetrical Nacelles Varied Chordwise at 40 Percent Semispan of a 45° Sweptback, Tapered Wing. NACA RM L50G17a, 1950.

3. Hoffman, Sherwood: Comparison of Zero-Lift Drag Determined by Flight Tests at Transonic Speeds of Pylon, Underslung, and Symmetrically Mounted Nacelles at 40 Percent Semispan of a 45° Sweptback Wing and Body Combination. NACA RM L51D26, 1951.

4. Pepper, William B., Jr., and Hoffman, Sherwood: Comparison of Zero-Lift Drags Determined by Flight Tests at Transonic Speeds of Symmetrically Mounted Nacelles in Various Chordwise Positions at the Wing Tip of a 45° Sweptback Wing and Body Combination. NACA RM L51F13, 1951.

5. Hoffman, Sherwood, and Mapp, Richard C., Jr.: Transonic Flight Tests to Compare the Zero-Lift Drags of 45° Sweptback Wings of Aspect Ratio 3.55 and 6.0 with and without Nacelles at the Wing Tips. NACA RM L51L27, 1952.

6. Hoffman, Sherwood, and Pepper, William B., Jr.: Transonic Flight Tests to Determine Zero-Lift Drag and Pressure Recovery of Nacelles Located at the Wing Tips on a 45° Sweptback Wing and Body Combination. NACA RM L51K02, 1952.

7. Abbott, Ira H.: Fuselage-Drag Tests in the Variable-Density Wind Tunnel: Streamline Bodies of Revolution, Fineness Ratio of 5. NACA TN 614, 1937.

8. Friedman, Morris D.: Arrangement of Bodies of Revolution in Supersonic Flow to Reduce Wave Drag. NACA RM A51I20, 1951.

[redacted]

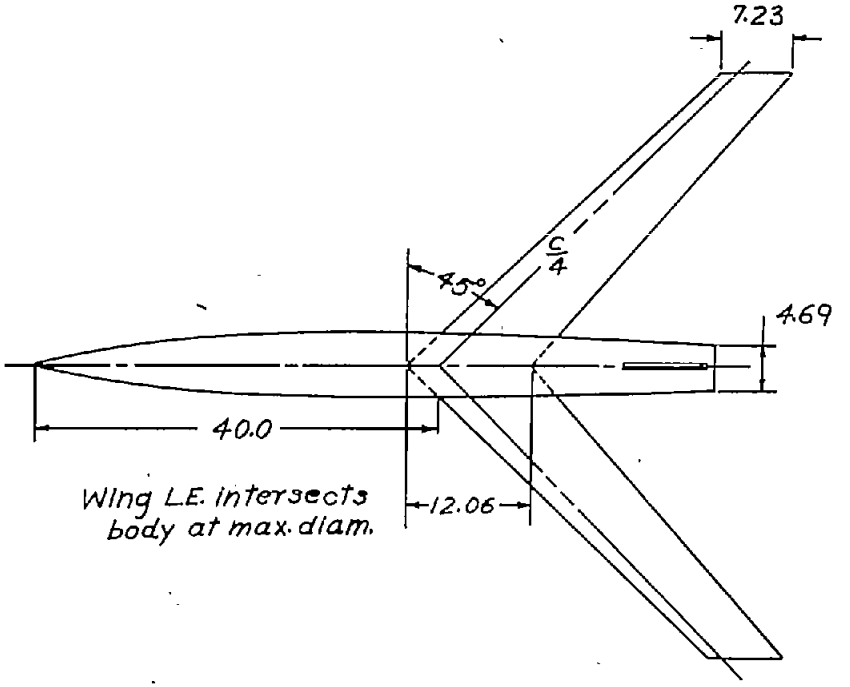

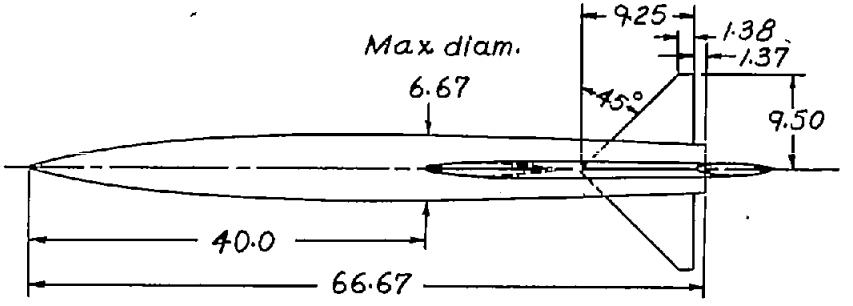

Model Characteristics:

Body fineness ratio	10.0
Wing aspect ratio	6.0
Wing taper ratio	0.6
Mean aerodynamic chord, ft	0.822
Airfoil parallel to free stream	NACA 65A009
Total wing plan-form area, sq ft	3.878
Exposed wing plan-form area, sq ft	3.333
Body frontal area, sq ft	0.242
Total frontal area, sq ft	0.650
Exposed fin plan-form area- two fins, sq ft	0.468

Fins are flat plates and 0.001 inch thick with 0.045-inch radius at edges.

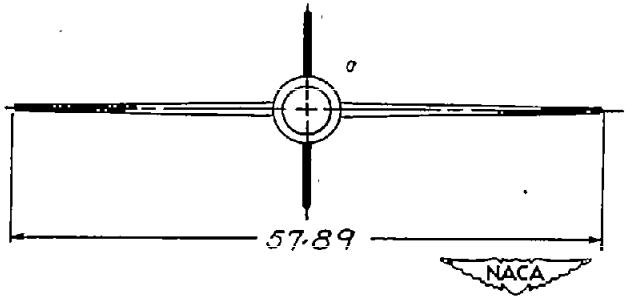

Figure 1.- General arrangement and dimensions of test model (model A). All dimensions are in inches.

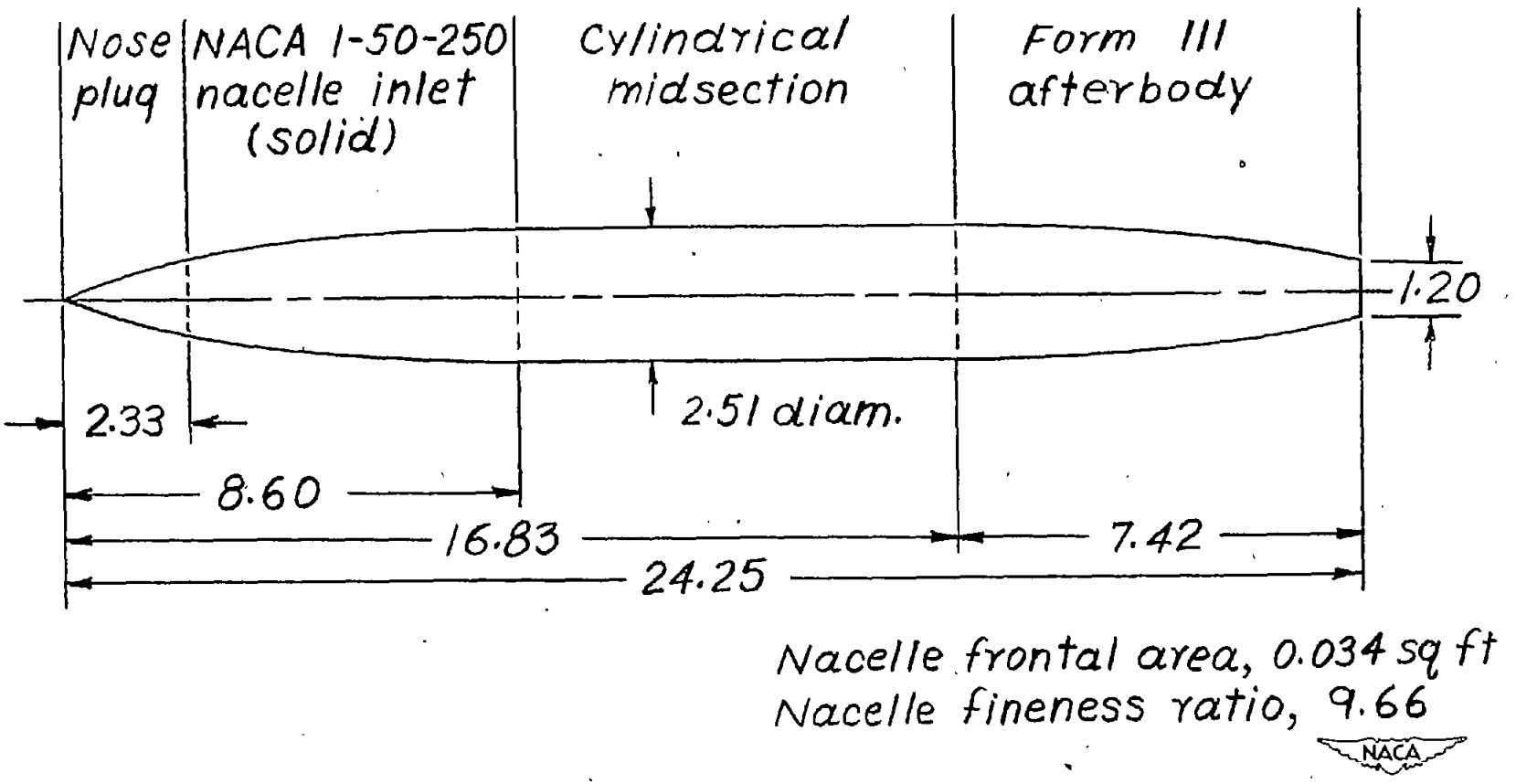

Figure 2.- Details and dimensions of solid nacelle. All dimensions are in inches.

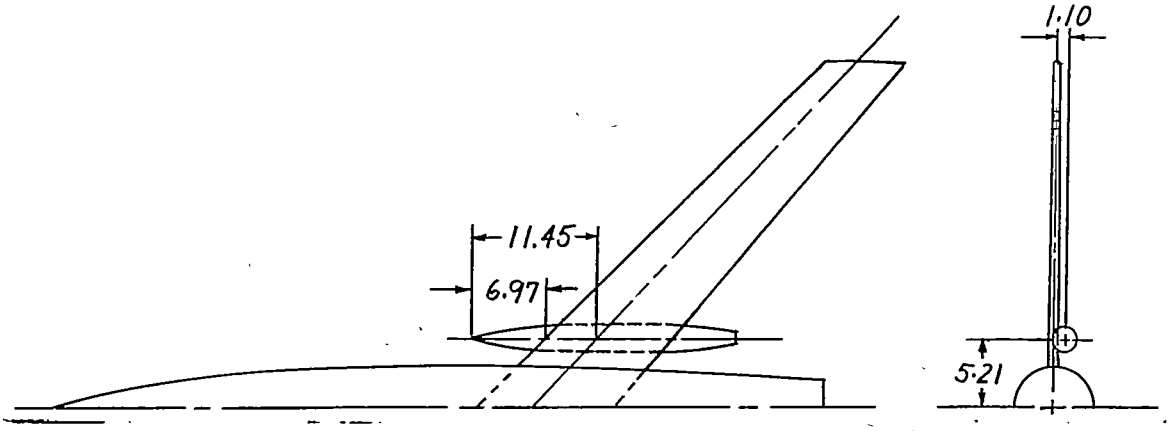

(a) Underslung nacelles at 18-percent semispan (model B).

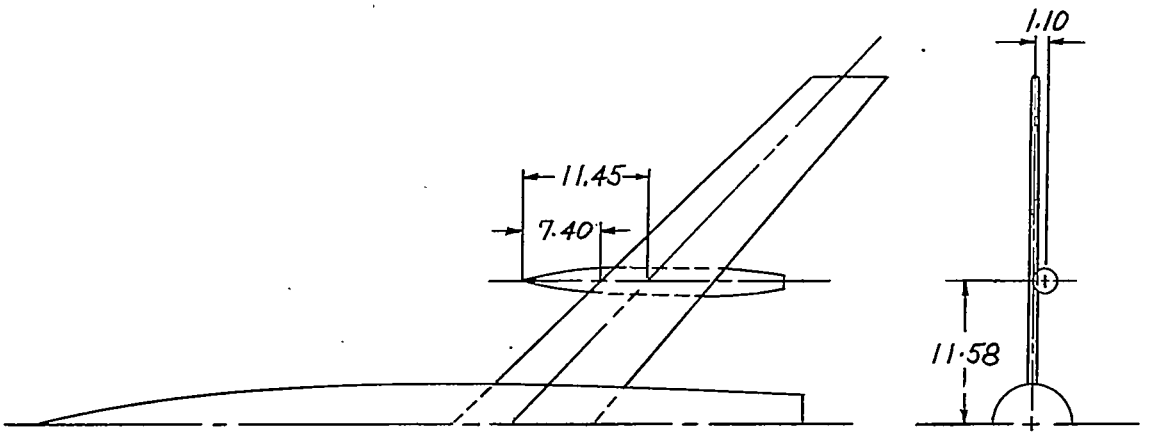

(b) Underslung nacelles at 40-percent semispan (model C).

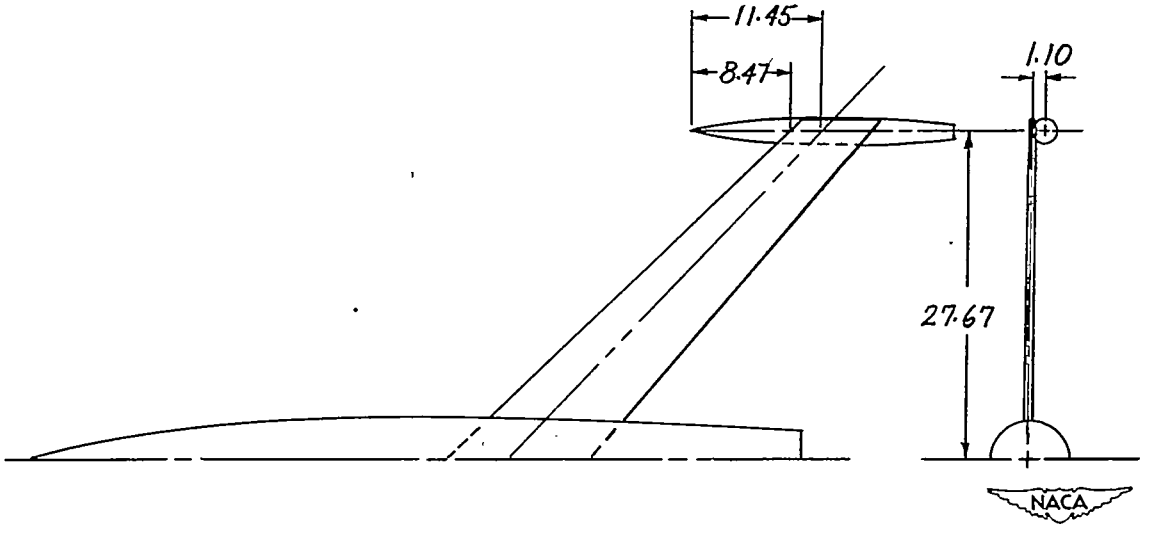

(c) Underslung nacelles at 96-percent semispan (model D).

Figure 3.- Comparison of nacelle locations on models. All dimensions are in inches.

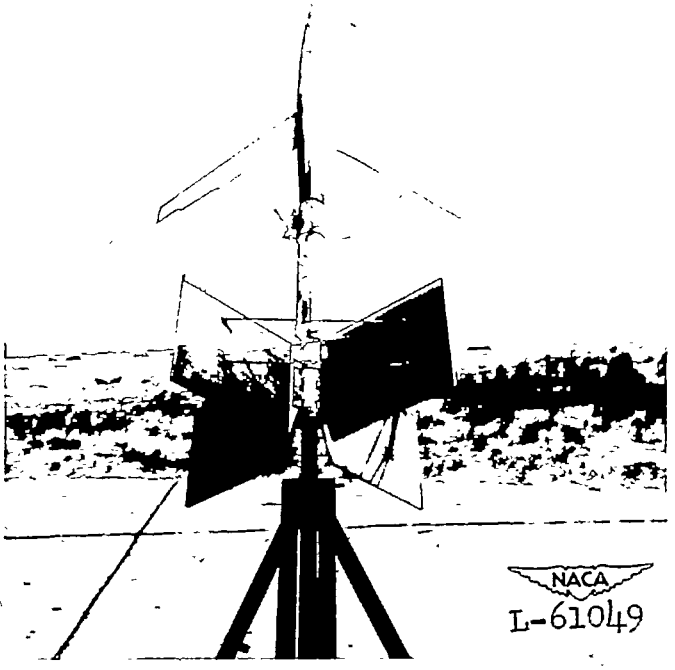

Model A

(a) Test model without nacelles. Model and booster arrangement on rail launcher.

Figure 4.- General views of test models.

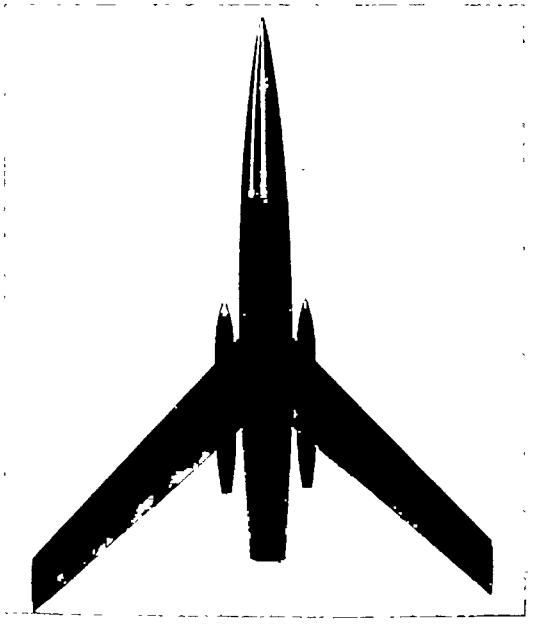

Model B; $\frac{y}{b/2} = 0.18$

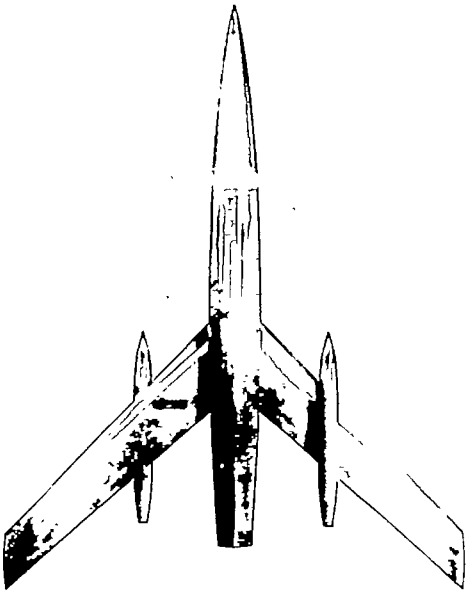

Model C; $\frac{y}{b/2} = 0.40$

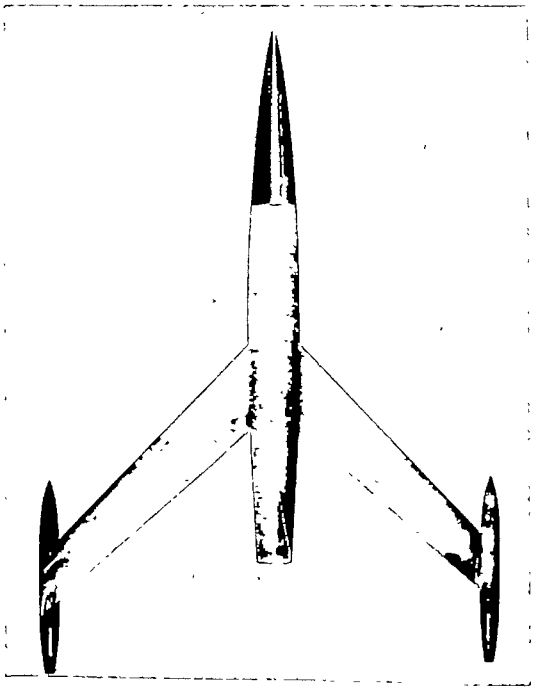

Model D; $\frac{y}{b/2} = 0.96$

(b) Test models with nacelles.

NACA L-75088

Figure 4.- Concluded.

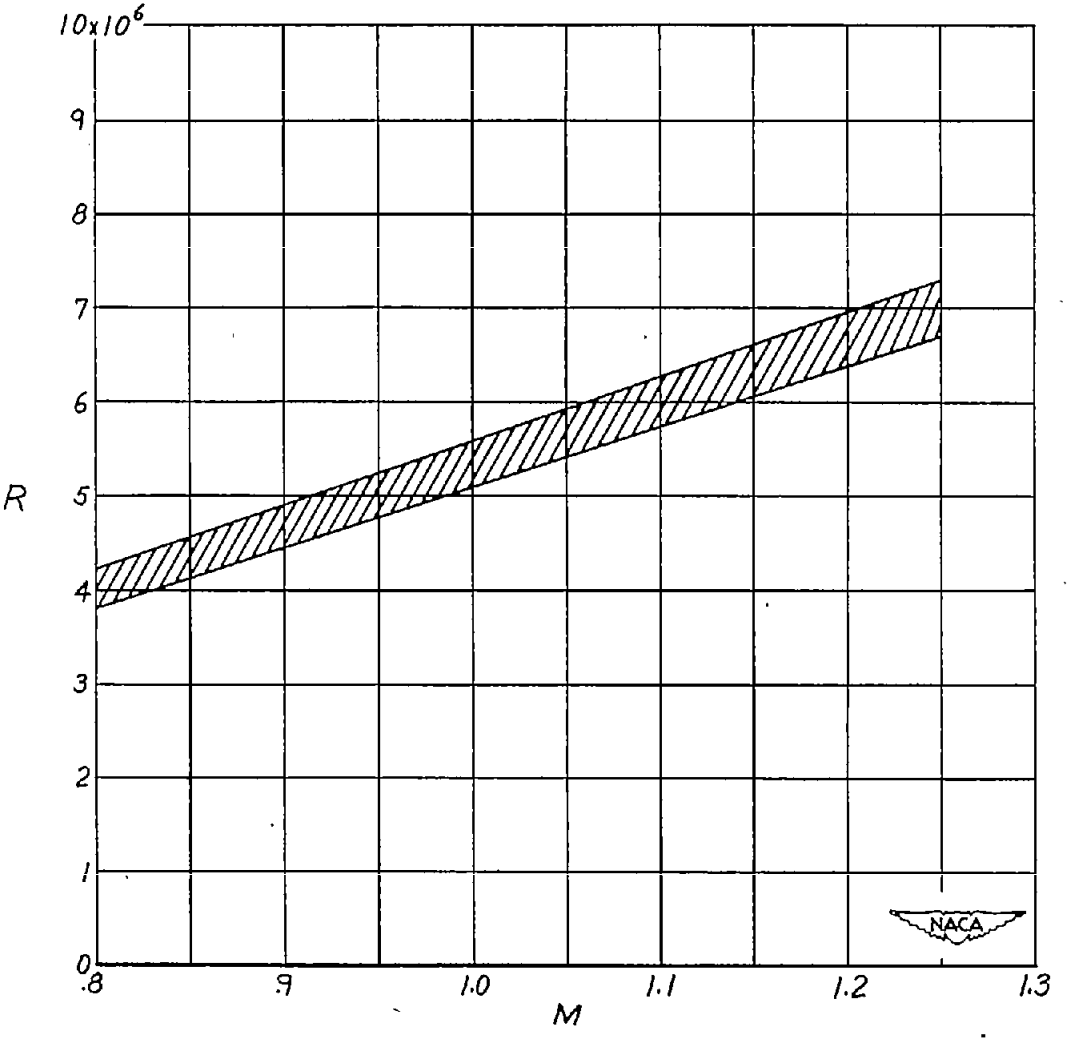

Figure 5.- Variation of Reynolds number with Mach number for models tested. Reynolds number based on wing mean aerodynamic chord.

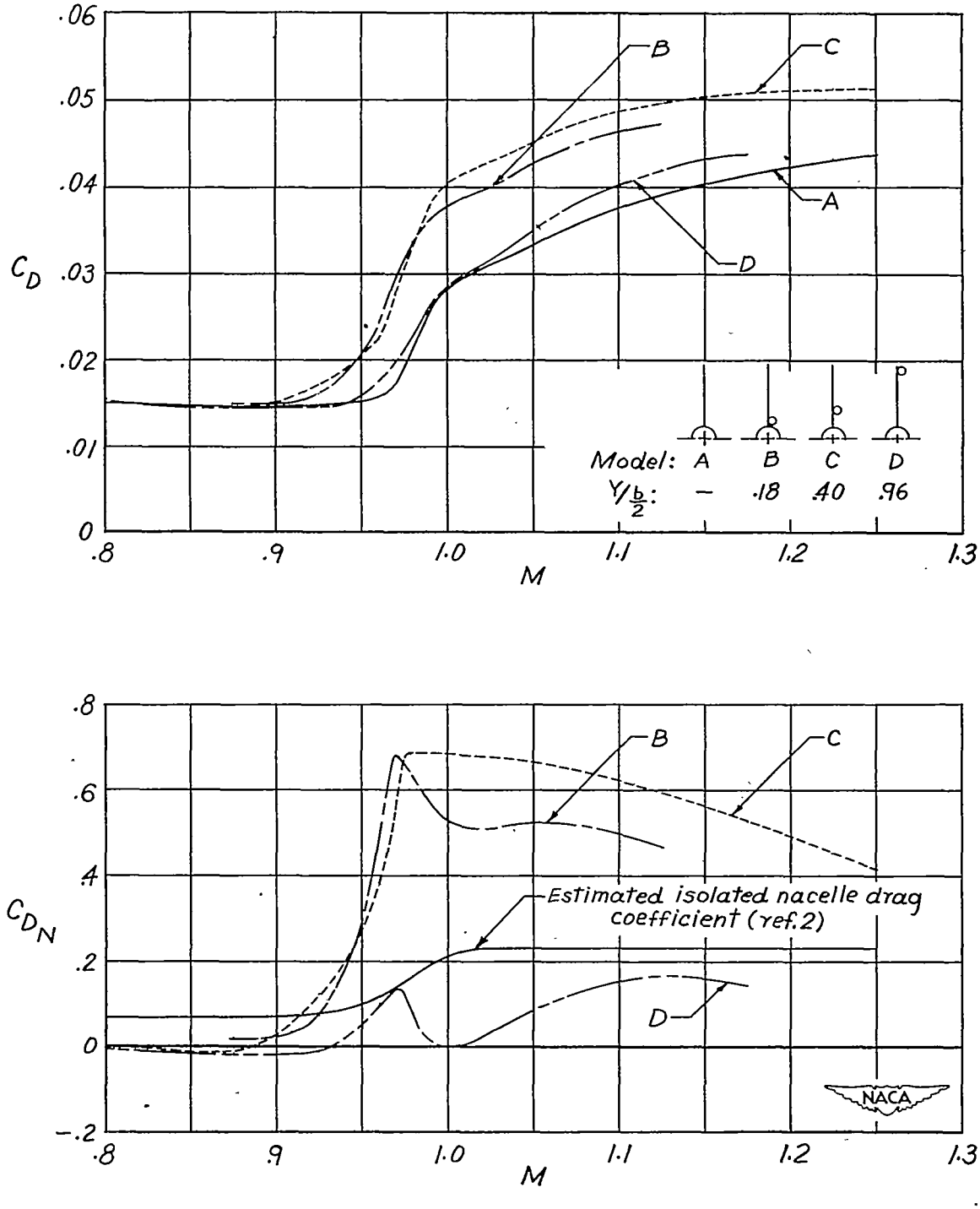

Figure 6.- Variation of total drag and nacelle-plus-interference drag coefficients with Mach number for models tested.

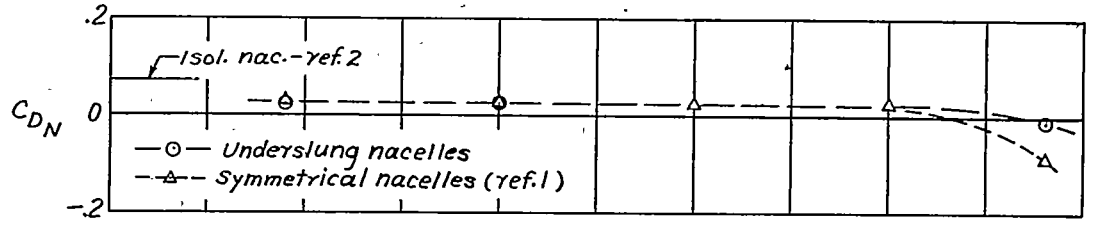

(a) M = 0.9.

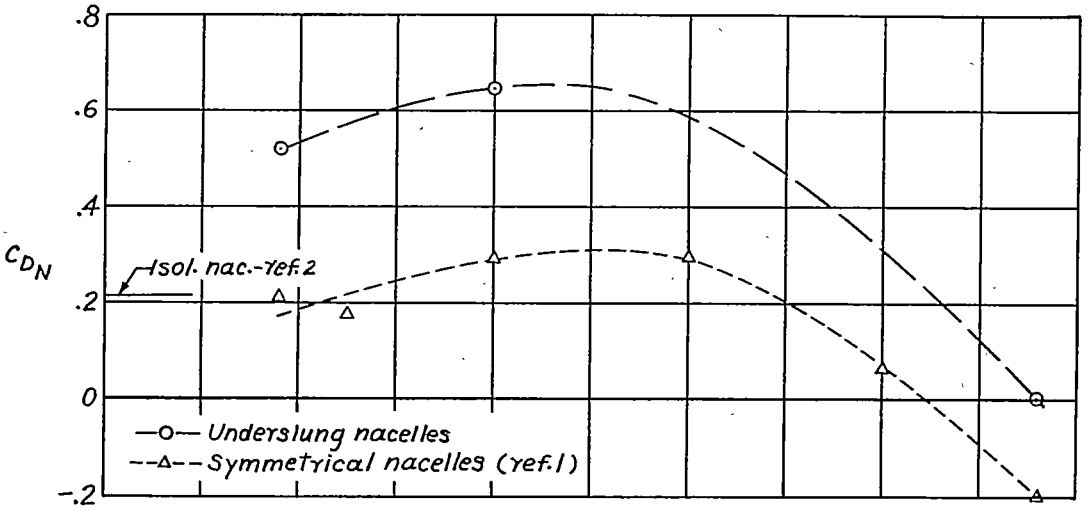

(b) M = 1.0.

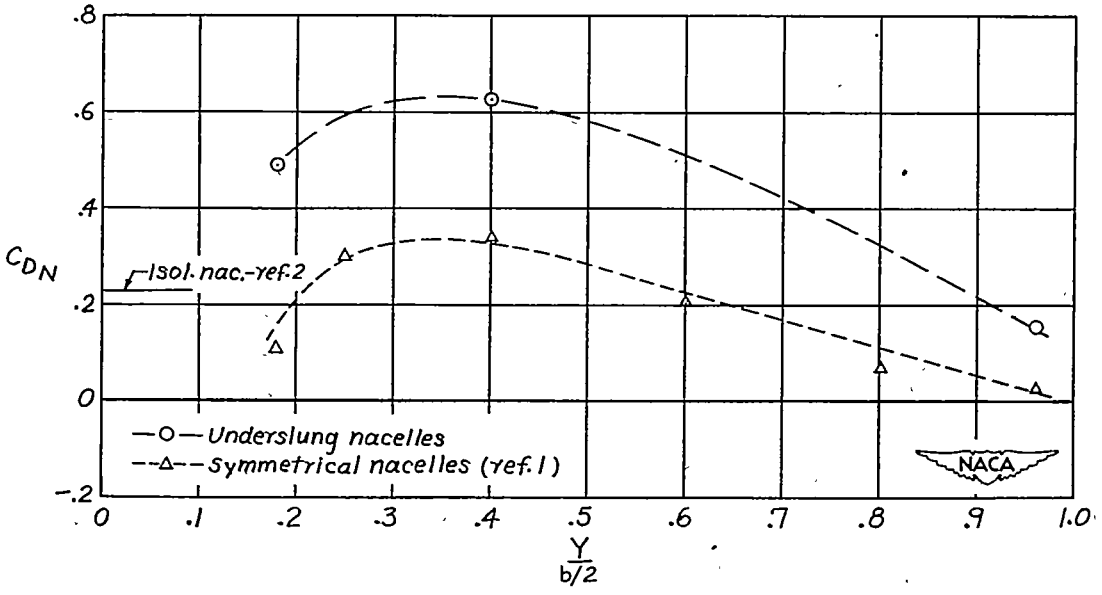

(c) M = 1.10.

Figure 7.- Comparisons of nacelle-plus-interference drag coefficients for underslung and symmetrically mounted nacelles (ref. 1) at Mach numbers of 0.9, 1.0, and 1.10.

[redacted]

NACA-Langley - 7-1-52 - 325